Log # TXX-92484
File # 10010
915

TUELECTRIC

October 12, 1992

William J. Cahill, Jr.
Group Vice President

U. S. Nuclear Regulatory Commission
Attn: Document Control Desk
Washington, DC 20555

SUBJECT: COMANCHE PEAK STEAM ELECTRIC STATION (CPSES)
DOCKET NOS. 50-445 AND 50-446
REQUEST FOR ADDITIONAL INFORMATION ON RXE-91-002
"REACTIVITY ANOMALY EVENTS METHODOLOGY"

REF: Teleconference between Mr. Tony Attard, NRC and Mr. Steve Maier, TU Electric dated August 11, 1992

Gentlemen:

In the above referenced conference call, additional analyses were discussed which would demonstrate the conservative nature of TU Electric's point kinetics analytical model of the Rod Ejection event. The additional analyses have been completed and are summarized in the attachment to this letter.

If clarification regarding the additional analyses is required, please contact Mr. Steve Maier at (214) 812-8229.

Sincerely,

William J. Cahill, Jr.

By: DRWoodlan
D. R. Woodlan
Docket Licensing Manager

DNB/dnb
Attachment

c - Mr. J. L. Milhoan, Region IV
Mr. T. A. Bergman, NRR
Mr. B. E. Holian, NRR
Resident Inspectors, CPSES (2)

140073

D029

TOPICAL REPORT RXE-91-002

REACTIVITY ANOMALY EVENTS METHODOLOGY

Note: The references, figures, tables, and nomenclature quoted in this response correspond to those provided in Topical Report RXE-91-002. References, figures, and tables within the text of this response that are not found within RXE-91-002 are identified by alphabetic character, and are located at the end of the response to this question.

Question

Please demonstrate the conservative nature of TU Electric's point kinetics analytical approach to the Control Rod Ejection (CRE) event by providing a comparison to the current CPSES Unit 1 CRE event analyses.

Answer

The TU Electric analytical methodology for the CRE event utilizes a point kinetics model to determine the core average power response. In contrast, the Westinghouse analytical methodology for the CRE event employs a one-dimensional (1-D) kinetics model to generate the core average power response. The CRE event results presented in the CPSES FSAR were generated using the Westinghouse 1-D approach. Westinghouse has previously demonstrated the conservatism of the 1-D approach with respect to a more detailed 3-D approach in WCAP-7588, Revision 1-A [26]. In addition, comparisons between the RETRAN point kinetics approach and the Westinghouse 1-D approach have concluded

that the RETRAN point kinetics approach compares favorably with the Westinghouse 1-D approach [A].

Four CRE event scenarios are presented in the CPSES FSAR. A comparison analysis was performed for each of these cases. The four cases analyzed are:

BOC HZP - Beginning-of-Cycle Hot Zero Power;
BOC HFP - Beginning-of-Cycle Hot Full Power;
EOC HZP - End-of-Cycle Hot Zero Power; and,
EOC HFP - End-of-Cycle Hot Full Power.

The important input parameters for each scenario are summarized in Table A-1.

Although the analytical results of all four cases are presented in the FSAR. plots of the results are available for only two cases - BOC HFP and EOC HZP. The plots available for each of these two cases include the normalized nuclear power history, and the fuel pellet centerline and radially-averaged temperatures at the core hot spot. It should be noted that the data points representing the FSAR curves are derived manually from the plots. Tables A-2 and A-3 provide a comparison between the RETRAN point kinetics and FSAR 1-D event response times for the BOC HFP and EOC HZP cases, respectively.

The calculated power histories for the BOC HFP scenario (Figure A-1) demonstrate that the peak core average fission power predicted by the 1-D and point kinetics models are nearly identical. In addition, the peak power for each model occurs at the same time, as shown in Table A-4. However, two noteworthy differences are evident.

The more significant of the two differences relates to the predicted power history after the release of the control rods following reactor trip signal (~0.35 second). The use of different methods for modelling the reactivity insertion caused by the control rods falling into the core after reactor trip causes the power histories to deviate. The methods employed by the 1-D kinetics model achieve greater accuracy for trip reactivity insertion by crediting the changes in the reactivity insertion rate as a function of the axial flux shape. The point kinetics model, on the other hand, must utilize a fixed table of reactivity versus time to conservatively represent the scram characteristics. This table is based on an axial flux distribution selected to provide a delayed insertion of the trip reactivity.

The less significant of the two differences pertains to the fact that the 1-D kinetics model tends to maintain the core power at a relatively high value longer than the point kinetics model prior to the insertion of the scram reactivity. A review of Figure A-2 indicates that the power deviation prior to the insertion of the scram reactivity does not substantially affect the total energy release for the BOC HFP case. Because the fuel temperature and enthalpy responses are a direct result of the integrated energy release, it can be concluded that the difference in core power levels prior to scram reactivity insertion has little impact on the event results.

The calculated centerline and radially-averaged fuel temperature histories for the BOC HFP scenario (Figures A-3 and A-4, respectively) also exhibit the impact of the delayed trip reactivity insertion modelling employed by the point kinetics model. The prolonged power generation predicted by the point kinetics model causes the fuel temperature to increase for a longer duration, and to

eventually peak at a much greater temperature. This increase in fuel temperature also results in a greater peak radially-averaged fuel enthalpy, as indicated in Table A-4.

The different centerline fuel temperatures predicted by the models can be attributed to two major differences in the hot spot modelling. The first of these differences is the result of the fuel pellet model used for the hot spot analysis. The fuel pellet model is selected to be consistent with the computer code used to generate the power distribution within the fuel pellet. The second of these differences is a consequence of the fuel pellet power distribution (PPD) chosen for use in the hot spot analysis. Westinghouse considers the calculated PPD to be proprietary information; thus, the specific values used by Westinghouse for the FSAR analysis are not available. In view of the fact that the initial fuel average temperatures are nearly the same, and that the PPD selection process employed by TU Electric considers the proper controlling factors (fuel exp re and initial enrichment), it can be concluded that the 1 centerline temperature predicted by TU Electric is appro iate.

As with the BOC HF cenario, the impact of the trip reactivity insertion model is evident for the EOC HZP scenario. Although the peak core fission power occurs at approximately the same time (see Table A-3), the peak power predicted by the point kinetics model is significantly greater than the response predicted by the 1-D kinetics model. The difference in peak power is great enough to result in a noticeable difference in the total energy release, as shown in Figure A-6. However, once the initial peak subsides, the energy release for the two cases increases at about the same rate until the time of trip reactivity insertion; the point kinetics model then predicts

a greater amount of total energy release. It can therefore be concluded that the initial power peak has the more significant impact on the HZP case, and that the point kinetics model predicts a greater peak power than the 1-D kinetics model.

The calculated centerline and radially-averaged fuel temperature histories for the EOC HZP scenario (Figures A-7 and A-8, respectively) also exhibit the impact of the core power history. The greater initial peak power, as predicted by the point kinetics model, results in a more prominent jump in fuel temperature during the initial phase of the event. The impact of the delayed trip reactivity insertion modelling employed by the point kinetics model is evident as a shift in the timing of the peak temperatures. As with the BOC HFP scenario, the increased fuel temperature also results in a greater peak radially-averaged fuel enthalpy, as indicated in Table A-[illegible].

As summarized in Table A-4, the TU Electric predicted responses to the FSAR event scenarios compare very well with the Westinghouse calculated responses. For the two cases where plotted data are available, the conservatism of the TU Electric methodology is quite evident. Based on these results, it can be concluded that the TU Electric Control Rod Ejection analytical methodology produces a more conservative core response than the Westinghouse analytical methodology.

REFERENCE

A. VEP-NFE-2-NP-A, "VEPCO Evaluation of the Control Rod Ejection Transient," Virginia Power Company, December 1984.

Table A-1

FSAR CRE Analysis Input Parameters

PARAMETER	TIME IN LIFE			
	BOC HZP	BOC HFP	EOC HZP	EOC HFP
Initial Power Level (%)	0	102	0	102
Ejected Control Rod Worth (pcm)	700	200	900	265
Doppler Weighting Factor	2.07	1.2	3.55	1.3
Doppler Reactivity Defect (pcm)	[(1)]	[(1)]	[(1)]	[(1)]
Moderator Temperature Coefficient (pcm)	+5.0	+5.0	[(1)]	[(1)]
Delayed Neutron Fraction, β_{EFF}	0.0055	0.0055	0.0044	0.0044
Prompt Neutron Lifetime(2) (10^{-6} seconds)	26.0	26.0	17.5	17.5
Trip Reactivity (pcm)	2000	4000	2000	4000
Time to Dashpot (seconds)	2.70	2.70	2.70	2.70
Pre-ejected Peak F_Q	--	2.50	--	2.50
Post-ejected Peak F_Q	13.0	4.43	20.0	5.41
Number of Operational RCPs(3)	2	4	2	4

(1) Westinghouse proprietary information

(2) Assumed value for point kinetics input

(3) Reactor Coolant Pumps

Table A-2

BOC HFP Sequence of Events

EVENT	TIME, seconds	
	TU Electric	FSAR
Initiation of Control Rod Ejection	0.00	0.00
Power Range High Neutron Flux High Setpoint Reached	0.05	0.05
Peak Nuclear Power Occurs	0.13	0.13
Control Rods Begin to Fall into Core	0.55	0.55
Peak Fuel Average Temperature Occurs	2.90	1.98

Table A-3

EOC HZP Sequence of Events

EVENT	TIME, seconds	
	TU Electric	FSAR
Initiation of Control Rod Ejection	0.00	0.00
Power Range High Neutron Flux Low Setpoint Reached	0.14	0.16
Peak Nuclear Power Occurs	0.17	0.18
Control Rods Begin to Fall into Core	0.64	0.66
Peak Fuel Average Temperature Occurs	1.46	1.51

Table A-4

Analysis Results Comparison

CASE ID	PARAMETER	TU ELECTRIC	FSAR
BOC HZP	PEAK FISSION POWER (FRACTION OF NOMINAL)	7.42	NOT REPORTED
	PEAK FUEL CENTERLINE TEMPERATURE, F	3725	3561
	PEAK FUEL AVERAGE TEMPERATURE, F	3246	3056
	PEAK FUEL AVERAGE ENTHALPY, cal/gm	143	127
	% PINS IN DNB	≤2.9	≤10
	% CORE MELT	0	0
BOC HFP	PEAK FISSION POWER (FRACTION OF NOMINAL)	1.59	1.59[1]
	PEAK FUEL CENTERLINE TEMPERATURE, F	4835	4570
	PEAK FUEL AVERAGE TEMPERATURE, F	3643	3383
	PEAK FUEL AVERAGE ENTHALPY, cal/gm	169	143
	% PINS IN DNB	≤0.01	≤10
	% CORE MELT	0	0
EOC HZP	PEAK FISSION POWER (FRACTION OF NOMINAL)	64.7	30.0[1]
	PEAK FUEL CENTERLINE TEMPERATURE, F	4238	3718
	PEAK FUEL AVERAGE TEMPERATURE, F	3807	3296
	PEAK FUEL AVERAGE ENTHALPY, cal/gm	174	139
	% PINS IN DNB	≤7.3	≤10
	% CORE MELT	0	0
EOC HFP	PEAK FISSION POWER (FRACTION OF NOMINAL)	2.34	NOT REPORTED
	PEAK FUEL CENTERLINE TEMPERATURE, F	4844	4642
	PEAK FUEL AVERAGE TEMPERATURE, F	3851	3458
	PEAK FUEL AVERAGE ENTHALPY, cal/gm	184	147
	% PINS IN DNB	≤0.02	≤10
	% CORE MELT	0.028	0

[1] Estimated from FSAR plot

Figure A-1 BOC HFP Core Average Fission Power Response

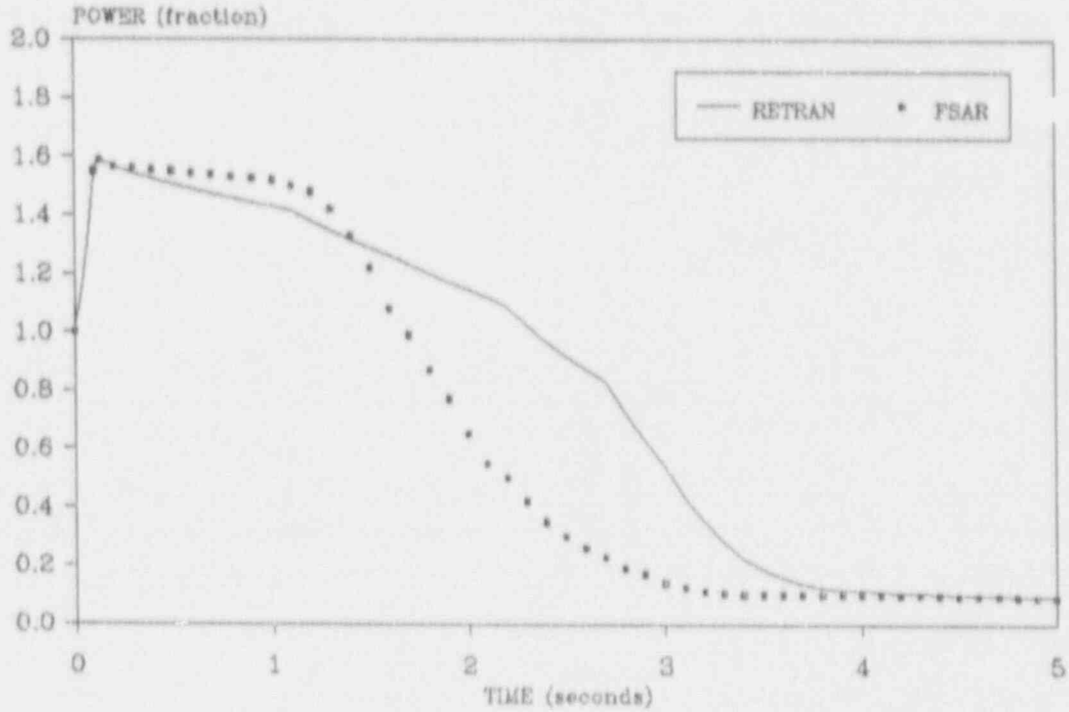

Figure A-2 BOC HFP Energy Release Response

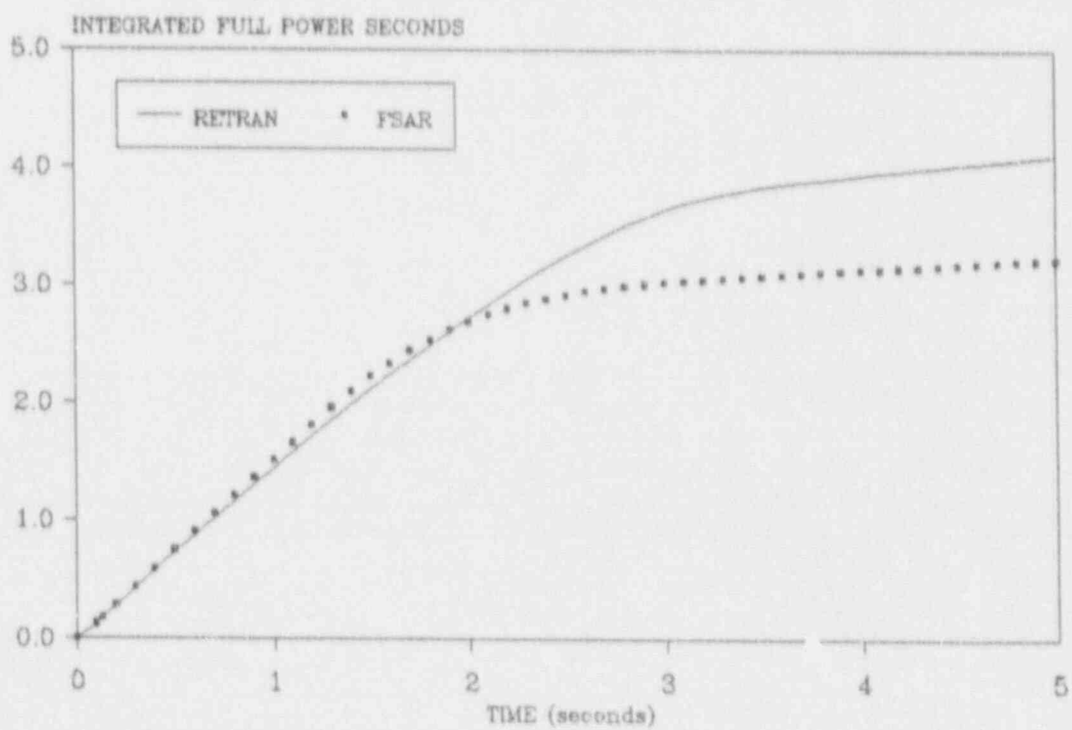

Figure A-3 BOC HFP Fuel Centerline Temperature Response

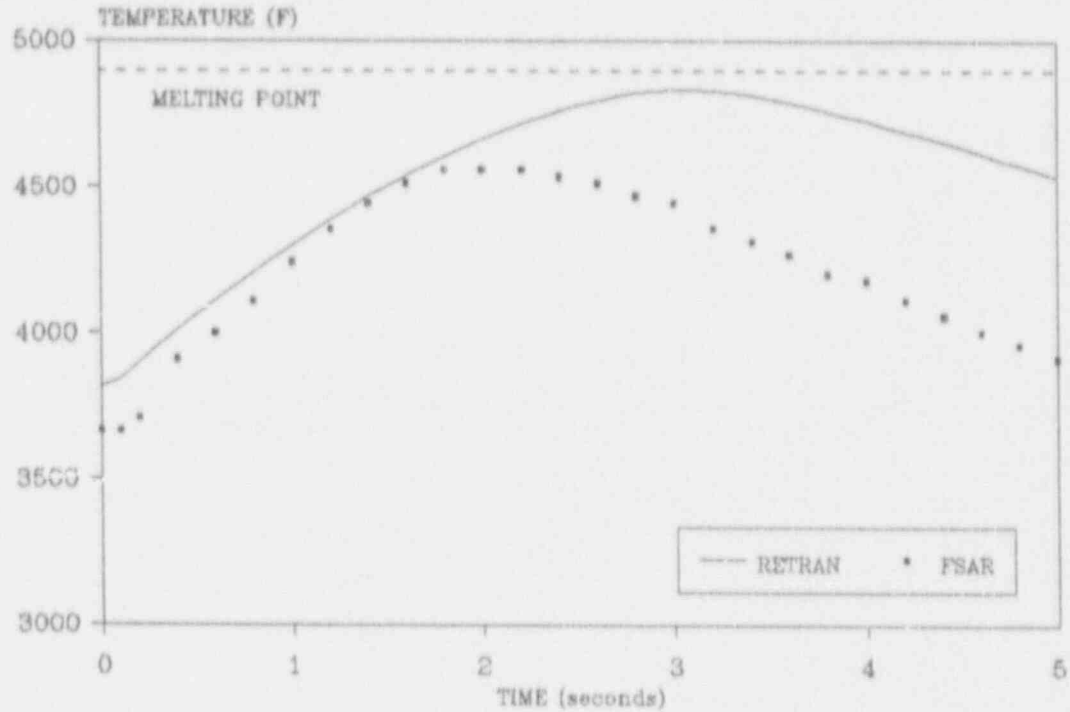

Figure A-4 BOC HFP Average Fuel Temperature Response

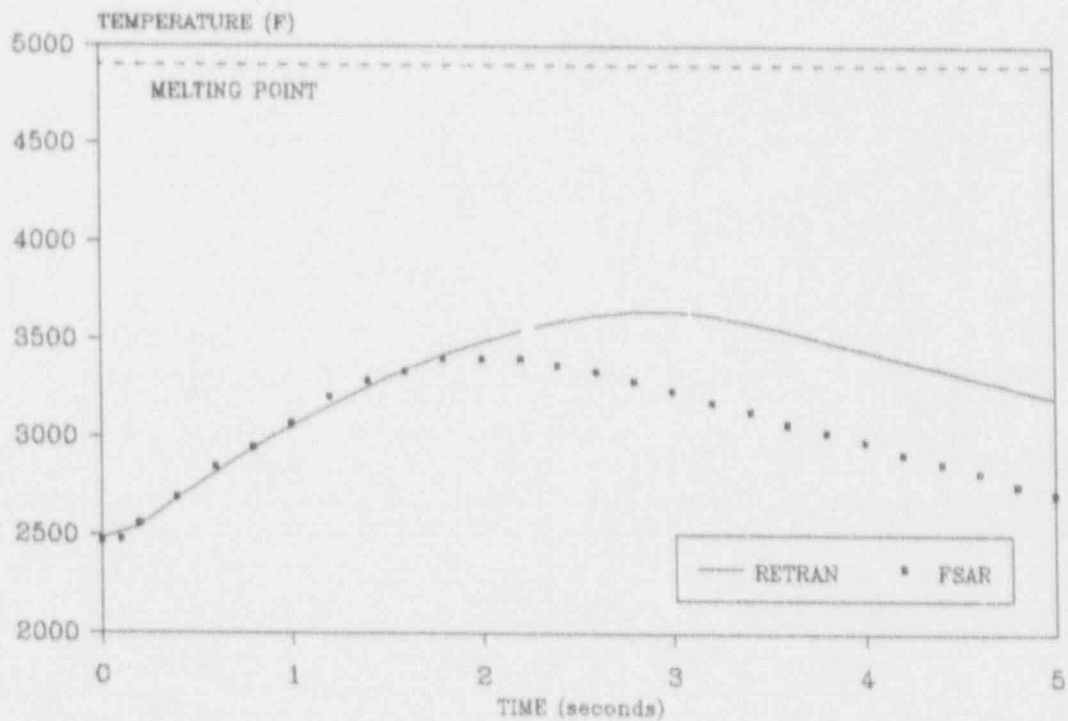

Figure A-5 EOC HZP Core Average Fission Power Response

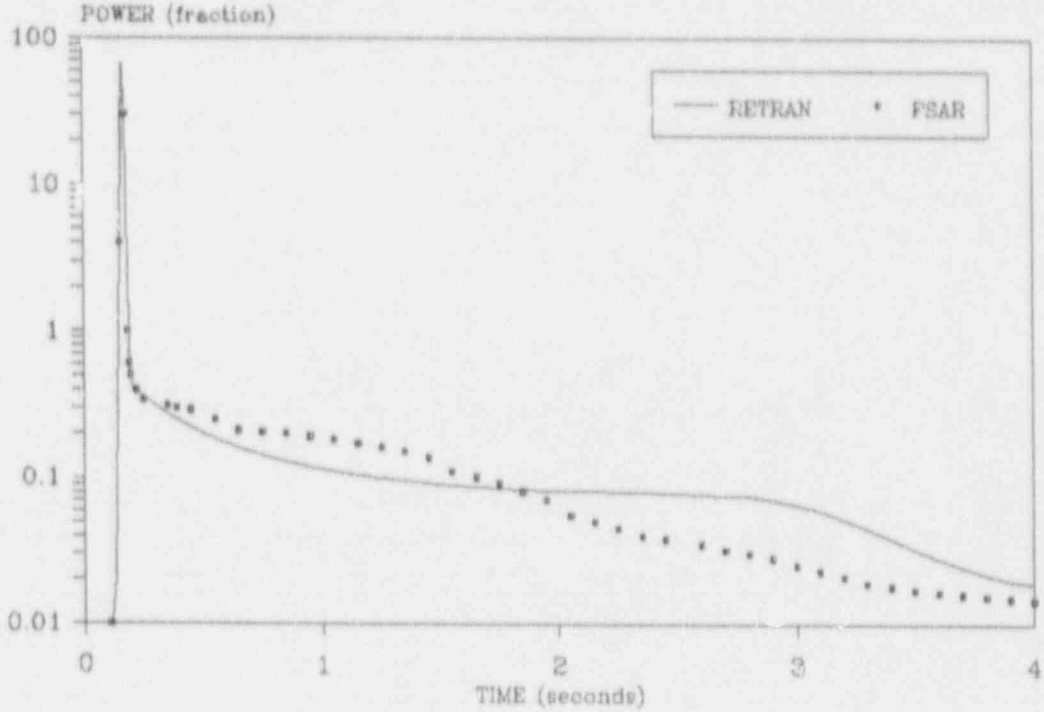

Figure A-6 EOC HZP Energy Release Response

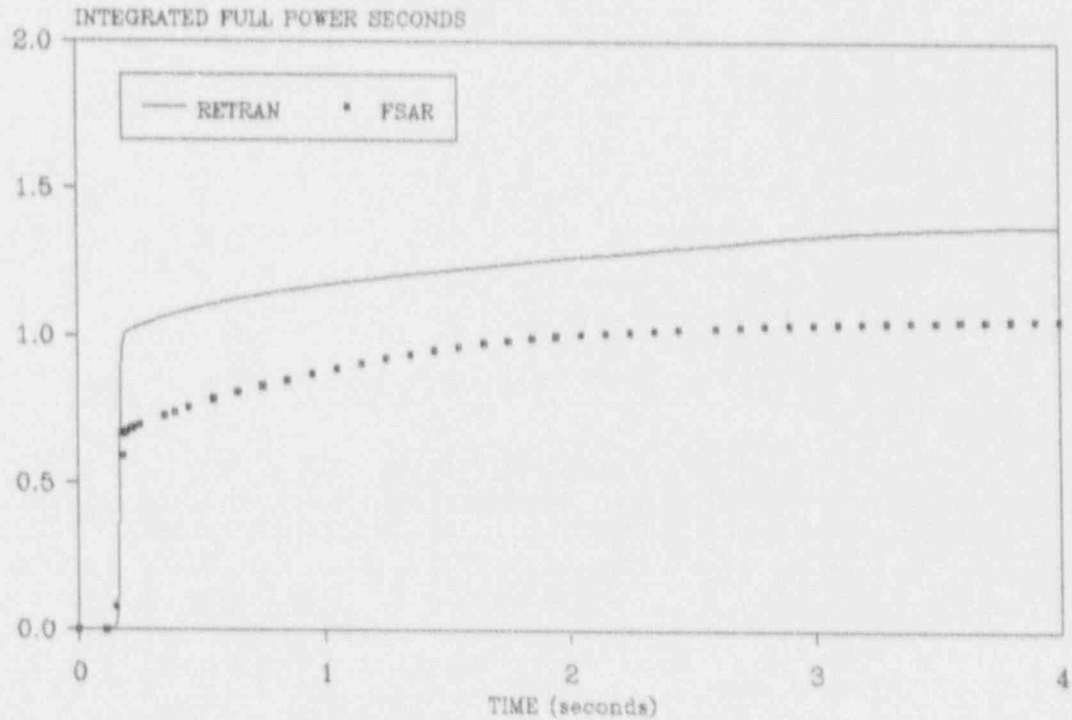

Figure A-7 EOC HZP Fuel Centerline Temperature Response

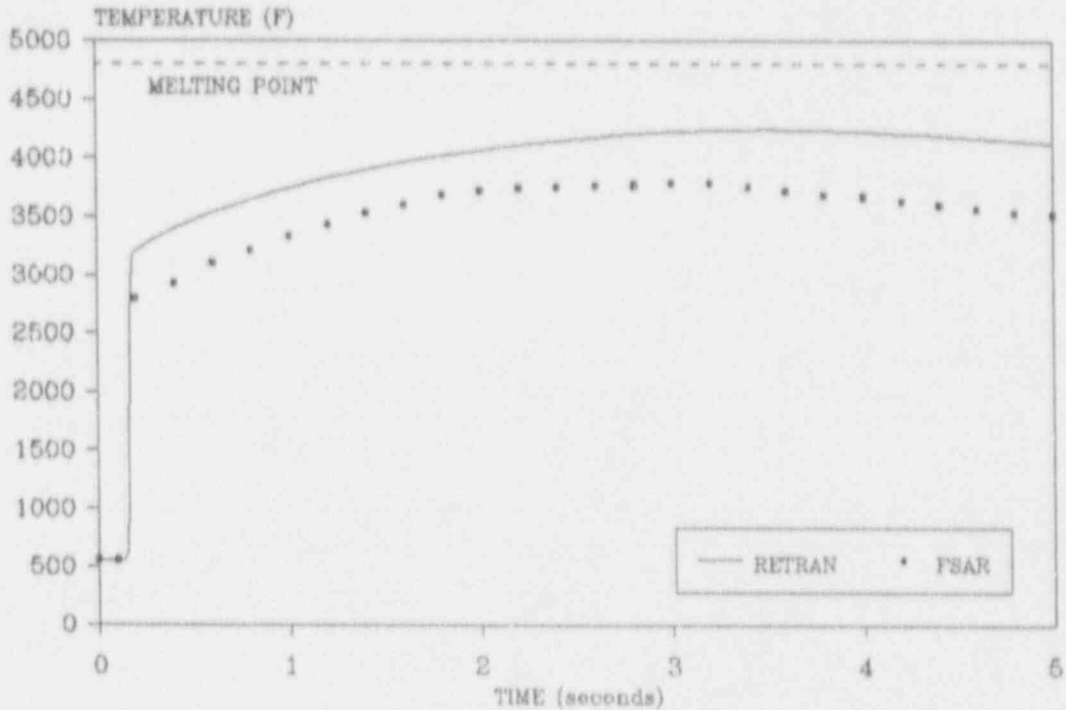

Figure A-8 EOC HZP Average Fuel Temperature Response